# Supporting Information

## A stable metal-organic framework with suitable pore sizes and rich uncoordinated nitrogen atoms on the internal surface of microspores for highly efficient $CO_2$ capture

Shao-Juan Bao,[a] Rajamani Krishna,[c] Ya-Bing He,[d] Jun-Sheng Qin,[a] Zhong-Min Su,*[a] Shun-Li Li,[a] Wei Xie,[a] Dong-Ying Du,*[a], Wen-Wen He,[a] Shu-Ran Zhang[a] and Ya-Qian Lan*[a,b]

[a] Institute of Functional Material Chemistry, Faculty of Chemistry, Northeast Normal University, Changchun 130024, P. R. China. E-mail: zmsu@nenu.edu.cn

[b] School of Chemistry and Materials Science, Nanjing Normal University, Nanjing 210023, P. R. China. E-mail: yqlan@njnu.edu.cn.

[c] Van't Hoff Institute for Molecular Sciences, University of Amsterdam Science Park 904, 1098 XH Amsterdam (The Netherlands).

[d] College of Chemistry and Life Sciences, Zhejiang Normal University, Jinhua 321004, China.

## S1. Materials and measurements

All the chemicals were obtained from commercial sources, and were used without further purification. Deionized water was used for all experiments. Elemental analyses (C, H and N) were measured on a Perkin-Elmer 2400 CHN elemental analyzer. IR spectrum was performed in the range 4000–400 $cm^{-1}$ using KBr pellets on an Alpha Centaurt FT/IR spectrophotometer. The X-ray powder diffraction (XRPD) data were carried out on a Siemens D5005 diffractometer with Cu-$K_\alpha$ ($\lambda$ = 1.5418 Å). Thermogravimetric analysis (TGA) was recorded on a Perkin-Elmer TG-7 analyzer under nitrogen heated from room temperature to 800 ºC at the heating rate of 5 °C·$min^{-1}$.

### S1.1 Synthesis of NENU-520

A mixture of $H_2L$ (30 mg, 0.11 mmol) and $Zn(NO_3)_2·6H_2O$ (150 mg, 0.50 mmol) was dissolved in a mixture of DMF/EtOH (6 mL/1.5 mL) and droped 0.01 mL $HNO_3$. The mixture was sealed in a 25 mL Teflon-lined autoclave and then heated at 90 °C for 3 days, then cooled to room temperature at 5 °C·$h^{-1}$. Colorless crystals **NENU-520** were collected and washed with DMF for several times (yield 40%, based on $H_2L$). Elemental analysis for $C_{34}H_{30}N_{10}O_6Zn_2$ (805.42): Anal. Calc.: C 50.70; H 3.75; N 17.39. Found: C 50.82; H 3.66; N 17.46%. IR (KBr, $cm^{-1}$): 3430 (w), 1670 (s), 1608 (s), 1571 (s), 1550 (m), 1508 (w), 1459 (m), 1419 (s), 1319 (m), 1255 (w), 1182 (w), 1093 (m), 1006 (w), 840 (m), 788 (s), 768 (s), 680 (w), 523 (w), 424 (w).

### S1.2 X-ray single crystal structure determination

Single crystal X-ray diffraction data in this work were recorded on a Bruker APEXII CCD diffractometer with graphite-monochromated Mo Kα radiation ($\lambda$ = 0.71069 Å) at 293 K. Absorption corrections were applied using multi-scan technique. All the structures were solved by Direct Method of SHELXS-97 and refined by full-matrix least-squares techniques using the SHELXL-97 program within WINGX.[1] Non-hydrogen atoms were refined with anisotropic temperature parameters. The SQUEEZE program implemented in PLATON was used to remove these electron densities for **NENU-520**. Thus, all of electron densities from free solvent molecules have been “squeezed” out.[2] CCDC: 990058 (**NENU-520**) contain the supplementary crystallographic data for this paper. Crystal data are summarized in Table S1 in the Supplementary Information. These data can be obtained free of charge from the Cambridge Crystallographic Data Centre via www.ccdc.cam.ac.uk/data_request/cif.

### S1.3 Gas adsorption experiments

The $N_2$, $H_2$, $CH_4$ and $CO_2$ adsorption measurements were performed on an automatic volumetric adsorption equipment (Quantachrome Autosorb-iQ). Before gas adsorption measurements, the samples were immersed in methanol for 24 h, and the liquid was poured out. Fresh methanol was subsequently added, and the crystals were stay for an additional 24 h to remove the nonvolatile solvates (DMF). The extract was decanted and fresh methanol was added once more. The sample was collected by decanting and treated with dichloromethane similarly to remove methanol solvates. After the removal of dichloromethane by decanting, the sample was activated by drying under a dynamic vacuum at room temperature overnight. Before the measurement, the sample was dried again by using the 'outgas' function of the surface area analyzer for 12 h at room temperature.

### S1.4 Fluorescence study

The finely ground sample **NENU-520** (3 mg) was immersed in 3 mL of different organic solvents. The mixtures were treated by ultrasonication for 30 min, and then aged to form stable suspensions before the fluorescence study. Fluorescence of the samples was performed using a F-4600 FL Spectrophotometer ($\lambda_{ex}$ = 310 nm).

The finely ground sample **NENU-520** (3 mg) was immersed in 3 mL of DMF containing different concentrations of nitrobenzene. The mixtures were treated by ultrasonication for 30 min, and then aged to form stable suspensions before the fluorescence study. Fluorescence of the samples was performed using a F-4600 FL Spectrophotometer ($\lambda_{ex}$ = 310 nm).

## S2. Calculation procedures of selectivity from IAST

### S2.1 Fitting of pure component isotherms

The measured experimental data on e*xcess* loadings, $q^{excess}$, of the pure components $CO_2$, $CH_4$, and $N_2$ in **NENU-520**, were first converted to *absolute* loadings, $q$, using

$$q = q^{excess} + \frac{pV_{pore}}{ZRT} \qquad (1)$$

where $Z$ is the compressibility factor. The Peng-Robinson equation of state was used to estimate $Z$. The accessible pore volume for **NENU-520** is 0.2694 $cm^3/g$.

The isotherm data for $CO_2$, measured at 273 K and 298 K were fitted with the Langmuir-Freundlich model

$$q = q_{sat} \frac{bp^{\nu}}{1 + bp^{\nu}} \quad (2)$$

with $T$-dependent parameter $b$

$$b = b_0 \exp\left(\frac{E}{RT}\right) \quad (3)$$

For $CO_2$, $CH_4$ and $N_2$, the isotherm data at 298 K were fitted with the Langmuir parameters provided in Table S4. Figure S10 provides a comparison of the experimental isotherms in **NENU-520** with the isotherm fits. And the isotherm fits are excellent.

**S2.2 IAST calculations of adsorption selectivities and uptake capacities**

The selectivity of preferential adsorption of component 1 over component 2 in a mixture containing 1 and 2, perhaps in the presence of other components too, can be formally defined as

$$S_{ads} = \frac{q_1/q_2}{p_1/p_2} \quad (4)$$

In equation (4), $q_1$ and $q_2$ are the *absolute* component loadings of the adsorbed phase in the mixture. These component loadings are also termed the uptake capacities. We calculate the values of $q_1$ and $q_2$ using the Ideal Adsorbed Solution Theory (IAST) of Myers and Prausnitz.[3]

**S3. The isosteric heats of adsorption**

The isosteric heat of adsorption, $Q_{st}$, defined as

$$Q_{st} = RT^2 \left(\frac{\partial \ln p}{\partial T}\right)_q \quad (5)$$

were determined using the pure component isotherm fits using the Clausius-Clapeyron equation.

In equation (5), $P$ is pressure, $T$ is temperature, $q$ is the amount adsorbed, $R$ is the gas constant, and $Q_{st}$ denotes the heat of adsorption.

**S4. Transient breakthroughs in fixed bed adsorbers**

The performance of industrial fixed bed adsorbers is dictated by a combination of adsorption selectivity and uptake capacity. For a proper comparison of various MOFs, we perform transient breakthrough simulations using the simulation methodology described in the literature.[4-7] For the breakthrough simulations, the following parameter values were used: length of packed bed, $L$ = 0.3 m; voidage of packed bed,

$\varepsilon$ = 0.4; superficial gas velocity at inlet, $u$ = 0.04 m/s; see schematic in Figure 4. Ther framework density of **NENU-520** is 1318 kg $m^{-3}$.

The transient breakthrough simulation results are presented in terms of a *dimensionless* time, $\tau$, defined by dividing the actual time, $t$, by the characteristic contact time.

## S5. Supporting Figures

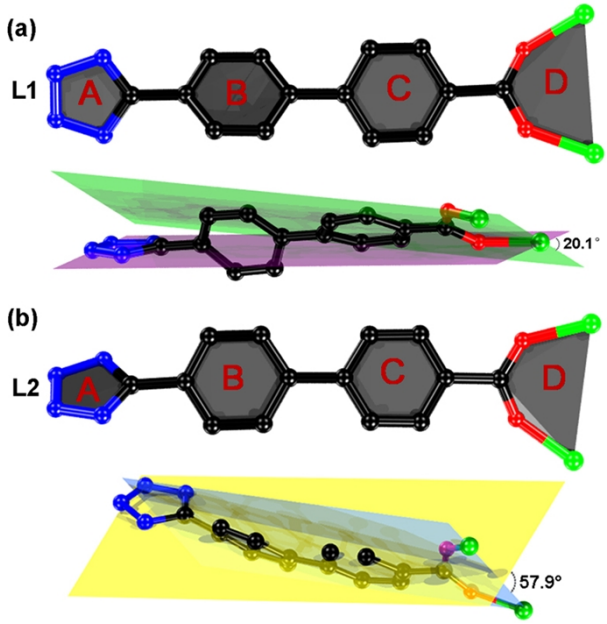


**Fig. S1** The coordination modes of two crystallographically distinct $L^{2-}$ fragments (L1 and L2) in **NENU-520**.

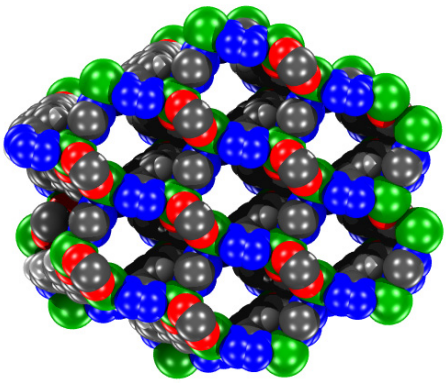

**Fig. S2** The spacefilling representation of the 3D open framework in **NENU-520**.

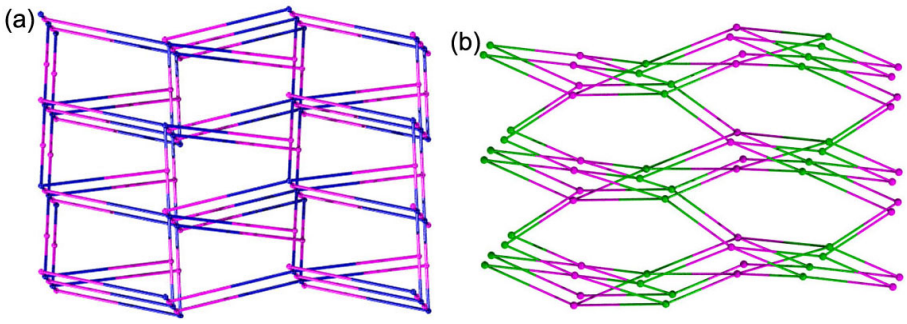


**Fig. S3** The (3,6)-connected (a) and the (4,4)-connected (b) topology net of **NENU-520**.

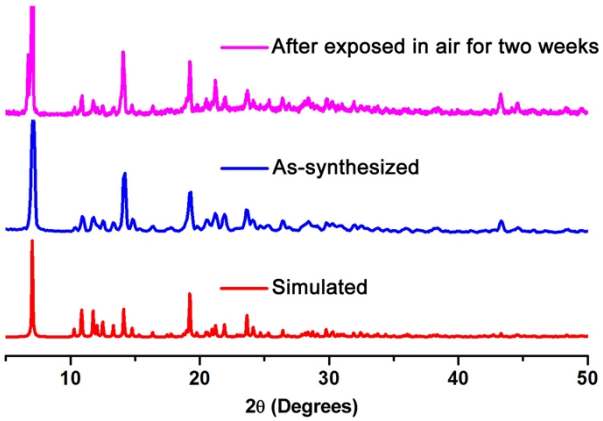


**Fig. S4** The XRPD patterns of **NENU-520**: the stimulated pattern (*red*), the as-synthesized sample (*blue*), and the as-synthesized sample in air for two weeks (*magenta*).

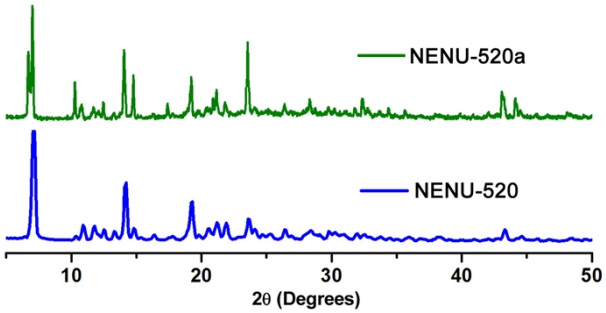


**Fig. S5** The XRPD patterns of the as-synthesized sample **NENU-520** in DMF (*blue*) and the activated sample **NENU-520a** (*green*).

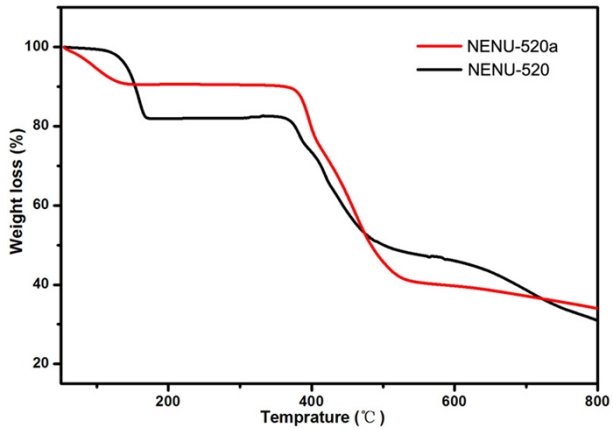


**Fig. S6** The TGA curve of **NENU-520** (*black*) and **NENU-520a** (*red*) measured under $N_2$ atmosphere from room temperature to 800 °C at the heating rate of 5 °C·min$^{-1}$.

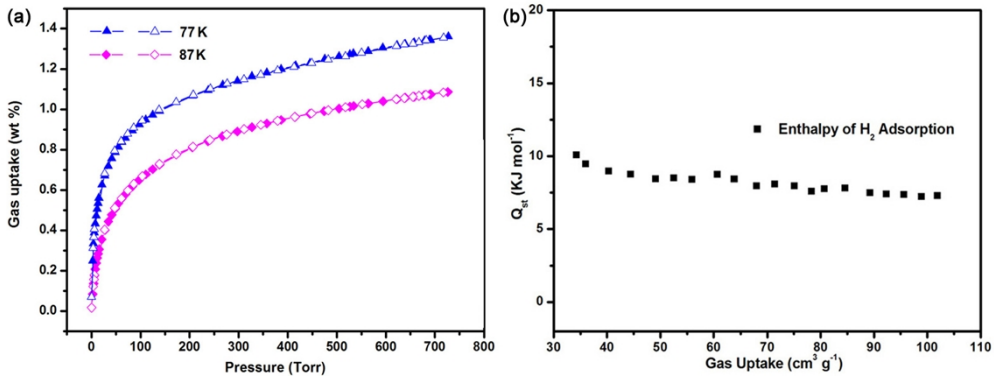


**Fig. S7** (a) $H_2$ sorption isotherms at 77 K (*blue*) and 87 K (*green*) for **NENU-520a**; (b) $Q_{st}$ of $H_2$ calculated by using the Clausius−Clapeyron equation for **NENU-520a**. (solid symbols, adsorption; open symbols, desorption).

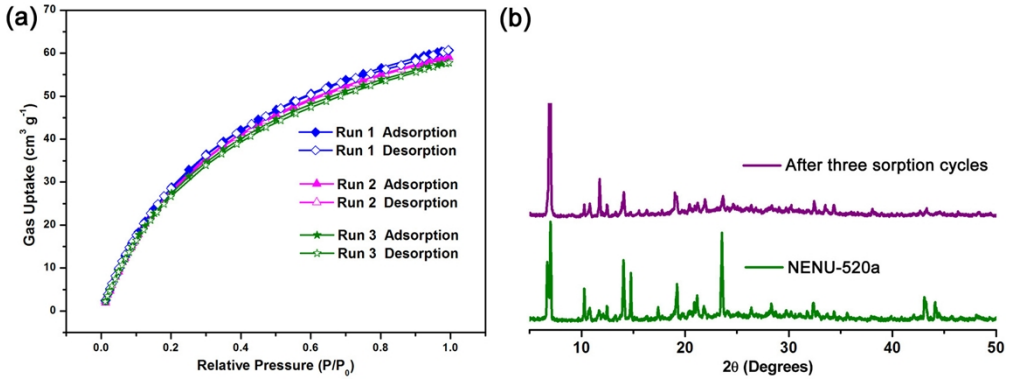


**Fig. S8** (a) The $CO_2$ sorption isotherms at 298 K for **NENU-520a** and (b) the PXRD pattern of the sample after three sorption cycles (*violet*).

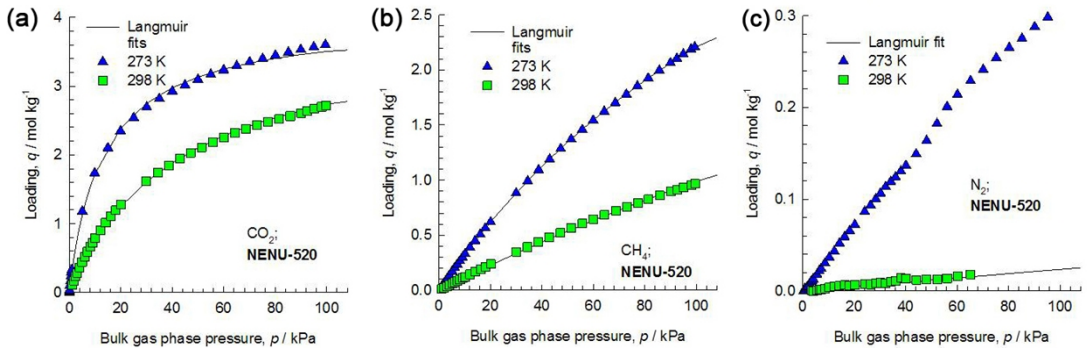


**Fig. S9** Comparison of the pure component isotherm data for (a) $CO_2$, (b) $CH_4$, and (c) $N_2$ in **NENU-520a** with the fitted isotherms (shown by continuous solid lines) at 273 K and 298 K.

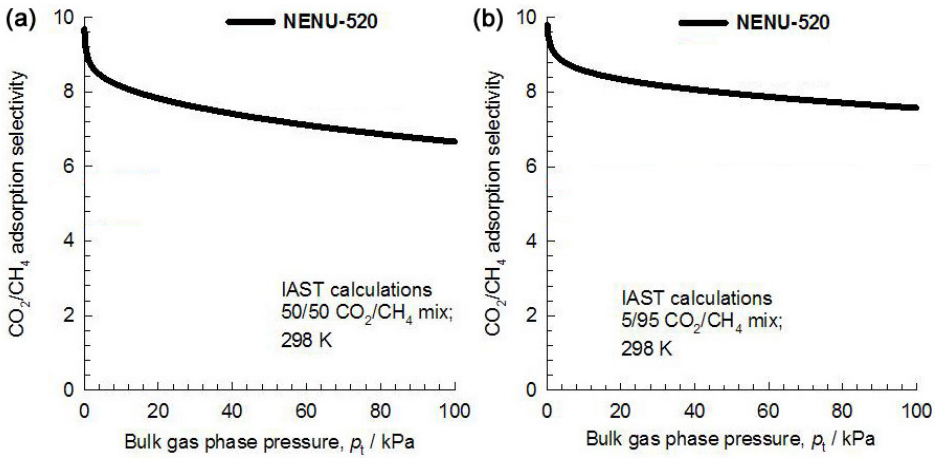


**Fig. S10** Calculations using Ideal Adsorbed Solution Theory (IAST) of Myers and Prausnitz[3] for adsorption selectivitites for (a) 50/50 $CO_2/CH_4$ and (b) 5/95 $CO_2/CH_4$ gas mixtures maintained at isothermal conditions at 298 K in **NENU-520**.

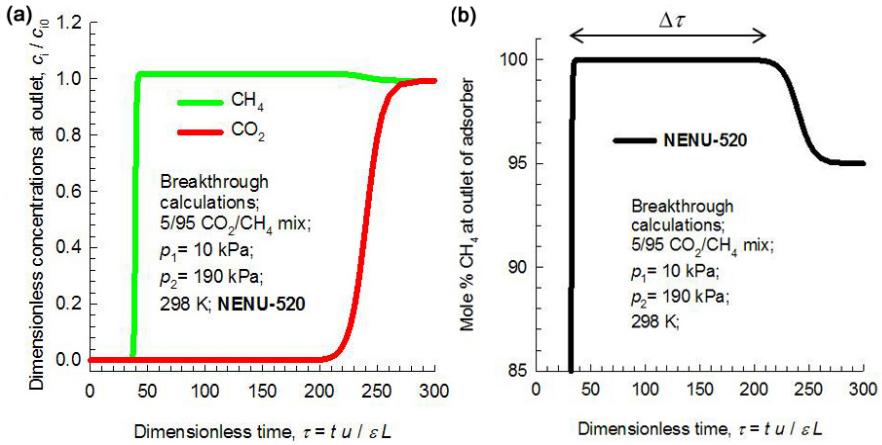


**Fig. S11** Breakthrough characteristics (a) and the mole percent $CH_4$ exiting (b) with 5/95 $CO_2/CH_4$ gas mixtures as a function of the dimensionless time in an adsorber packed with **NENU-520**. These calculations were at 200 kPa total pressure and 298 K.

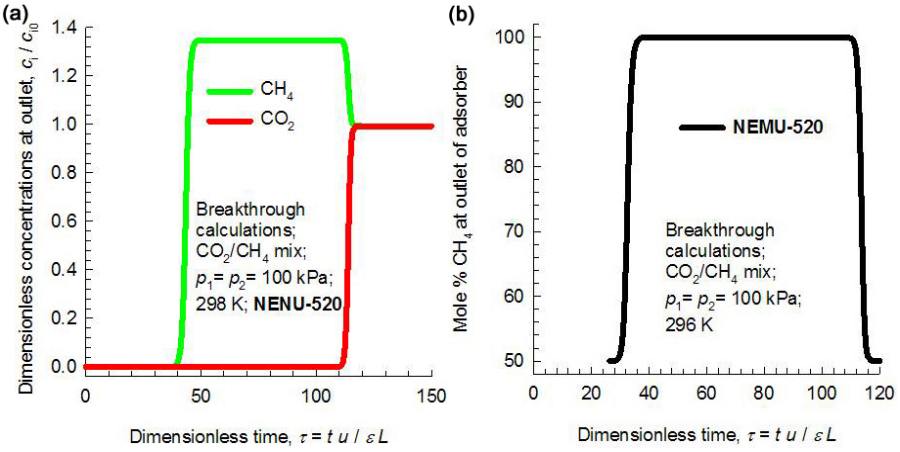

**Fig. S12** Breakthrough characteristics (a) and the mole percent $CH_4$ exiting (b) with 50/50 $CO_2/CH_4$ gas mixtures as a function of the dimensionless time in an adsorber packed with **NENU-520**. These calculations were at 200 kPa total pressure and 298 K.

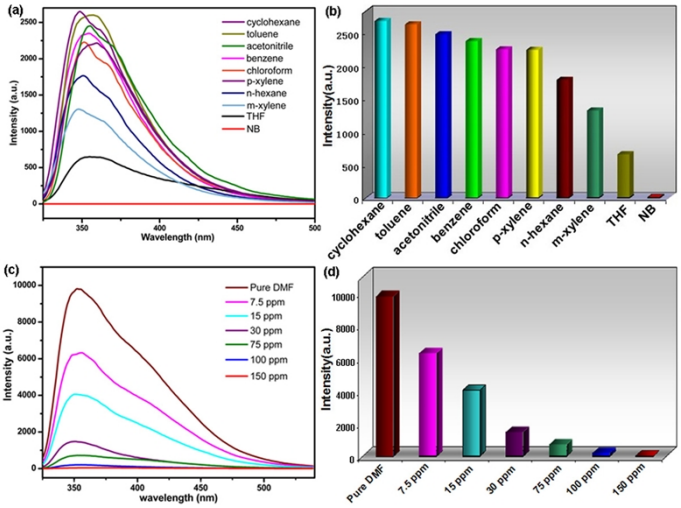


**Fig. S13** (a) and (b) Emission spectra and intensity of **NENU-520** in different organic solvents ($\lambda_{ex}$ = 310 nm, NB = nitrobenzene), (c) and (d) emission spectra and intensity of **NENU-520** in different concentrations of nitrobenzene in DMF ($\lambda_{ex}$ = 310 nm).

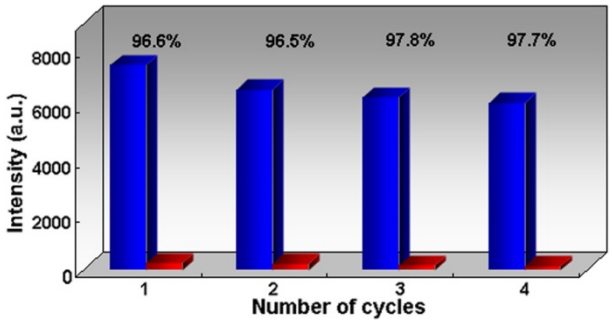


**Fig. S14** Quenching efficiency of **NENU-520** dispersed in DMF to 100 ppm nitrobenzene solution by centrifuging solution after use and washing several times with DMF.

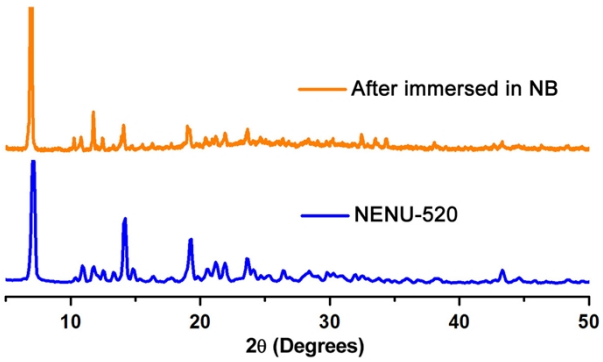


**Fig. S15** The XRPD spectra of **NENU-520**: the as-synthesized samples in DMF (*blue*), and after the detection of nitrobenzene (cycle 4, *orange*), respectively. After every cycle, the samples were centrifuged and washed with DMF for several times.

**Fig. S16** The FT/IR spectra of **NENU-520**: the as-synthesized samples in DMF (*black*), and after the detection of nitrobenzene (cycle 4, *green*). After every cycle, we centrifuged the solution and washed them with DMF for several times.

# S6. Notation

| | |
|---|---|
| $b$ | Langmuir-Freundlich constant for species $i$ at adsorption site A, $Pa^{-\nu_i}$ |
| $c_i$ | molar concentration of species $i$ in gas mixture, mol $m^{-3}$ |
| $c_{i0}$ | molar concentration of species $i$ in gas mixture at inlet to adsorber, mol $m^{-3}$ |
| $E$ | energy parameter, J $mol^{-1}$ |
| $L$ | length of packed bed adsorber, m |
| $p_i$ | partial pressure of species $i$ in mixture, Pa |
| $p_t$ | total system pressure, Pa |
| $q_i$ | component molar loading of species $i$, mol $kg^{-1}$ |
| $Q_{st}$ | isosteric heat of adsorption, J $mol^{-1}$ |
| $t$ | time, s |
| $T$ | absolute temperature, K |
| $u$ | superficial gas velocity in packed bed, m $s^{-1}$ |

## Greek letters

| | |
|---|---|
| $\varepsilon$ | voidage of packed bed, dimensionless |
| $\rho$ | framework density, kg $m^{-3}$ |
| $\nu$ | Freundlich exponent, dimensionless |
| $\tau$ | time, dimensionless |

## S7. Supporting Tables

**Table S1.** Crystal data and structure refinements for **NENU-520**.

| Empirical formula | $C_{34}H_{30}N_{10}O_6Zn_2$ |
|---|---|
| *M*w | 805.42 |
| Crystal system | Monoclinic |
| Space group | *Cc* |
| *a* (Å) | 8.3860(13) |
| *b* (Å) | 17.1990(15) |
| *c* (Å) | 25.132(4) |
| *β* (°) | 94.182(5) |
| *V* (Å$^3$) | 3615.2(9) |
| *Z* | 4 |
| $D_c$ (Mg·m$^{-3}$) | 1.476 |
| Abs.coeff. (mm$^{-1}$) | 1.385 |
| $R_{int}$ | 0.0321 |
| *F*(000) | 1640 |
| reflns collected | 11503 |
| Independent reflns | 6543 |
| GOF on $F^2$ | 1.018 |
| $R_1$[a] | 0.0470 |
| $wR_2$ (all data)[b] | 0.1205 |

[a] $R_1 = \Sigma||F_o| - |F_c||/\Sigma|F_o|$, [b] $wR_2 = |\Sigma w(|F_o|^2 - |F_c|^2)|/\Sigma|w(F_o^2)^2|^{1/2}$.

**Table S2.** The angles between the tetrazole rings and the benzene rings in **NENU-520**.

| Compound | Ligand | Two planes | Dihedral angle/° |
|---|---|---|---|
| **NENU-520** | L1 | AB | 54.8 |
| | | BC | 30.2 |
| | | AD | 20.1 |
| | L2 | AB | 43.6 |
| | | BC | 13.3 |
| | | AD | 57.9 |

**Table S3.** Gas adsorption data of **NENU-520a**.

| Temperature | Gas | Adsorption amount (at saturation) | | | | Number of molecules per unit cell |
|---|---|---|---|---|---|---|
| | | $cm^3\ g^{-1}$ | $cm^3\ cm^{-3}$ | $mmol\ g^{-1}$ | wt % | |
| 77 K | $N_2$ | 151.5 | 199.7 | 6.76 | 18.9 | 19.4 |
| | $H_2$ | 152.4 | 200.9 | 6.80 | 1.36 | 19.5 |
| 87 K | $H_2$ | 121.6 | 160.3 | 5.42 | 1.09 | 15.5 |
| 273 K | $CO_2$ | 80.43 | 106.0 | 3.59 | 15.7 | 10.3 |
| | $CH_4$ | 31.30 | 41.3 | 1.39 | 2.24 | 4.0 |
| | $N_2$ | 6.589 | 8.7 | 0.29 | 0.82 | 0.8 |
| 298 K | $CO_2$ | 60.64 | 79.9 | 2.71 | 11.9 | 7.8 |
| | $CH_4$ | 21.41 | 28.2 | 0.96 | 1.53 | 2.8 |
| | $N_2$ | 0.23 | 0.29 | 0.012 | 0.029 | 0.035 |

**Table S4**. Langmuir-Freundlich parameters for adsorption of $CO_2$, $CH_4$ and $N_2$ at 298 K in **NENU-520**.

| | $q_{sat}$ mol $kg^{-1}$ | $b_0$ $Pa^{-\nu}$ | $\nu$ dimensionless |
|---|---|---|---|
| $CO_2$ | 4 | $7.53\times10^{-11}$ | 0.97 |
| $CH_4$ | 6.2 | $1.56\times10^{-11}$ | 1 |
| N2 | 1 | $2.41\times10^{-7}$ | 1 |

**Table S5.** Comparison of IAST-Calculated Selectivity for $CO_2/CH_4$ and $CO_2/N_2$ Mixture in Different Porous Materials.

| Common names | $CO_2$ capacity | | $CO_2/CH_4$ (Composition and Temperature) | $CO_2/N_2$ (Composition and Temperature) | Reference |
|---|---|---|---|---|---|
| | 273 K | 298 K | 298 K | 298 K | |
| **NENU-520** | **80.43 $cm^3/g$ 106.0 $cm^3/cm^3$ 3.59 mmol/g 15.7 wt%** | **60.64 $cm^3/g$ 79.9 $cm^3/cm^3$ 2.71 mmol/g 11.9 wt%** | **14.1[a] 12.8[b]** | **400[c]** | **In this work** |
| SIFSIX-3-Zn | | 90 $cm^3/cm^3$ | 231[b] | 1818 (10/90) | *Nature,* 2013, **495**, 80-84. |
| Cu(bcppm)$H_2$O | | 1.04 mmol $g^{-1}$ (293 K) | | 590[c] (293K) | *J. Am. Chem. Soc*., 2013, **135**, 10441-10448. |
| UTSA-16 | | 160 $cm^3/cm^3$ (296 K) | | 314.7[c] (296 K) | *Nat Commun,* 2012, ***3,*** 954-963 |
| MAF-66 | 140 $cm^3/g$ | 99 $cm^3/g$ | 5.8 | 225[b] | *Inorg. Chem*., 2012, **51**, 9950−9955. |
| $[Cu(tba)_2]_n$ | 51.8 $cm^3/g$ | 43.9 $cm^3/g$ | 45[c] (293 K, 1 bar) | 45[c] (293 K, 1 bar) | *J. Am. Chem. Soc*., 2014, ***136***, 10906-10909. |
| [Zn(btz)]·DMF·0.5$H_2O$ | 98 $cm^3/g$ | | | | *J. Am. Chem. Soc*., 2012, **134**, 784- 787. |
| P5-SOF | | 8.8 wt% | 375 | 339 | *Adv. Mater*., DOI: 10.1002/adma.201401672. |
| Zn(HL)·$H_2O$]·DMA | 0.93 mmol g-1 | | | | *Chem. Commum.,* 2014, **50**, 6886-6889. |
| MAF-23 | 74.2 $cm^3/g$ | 56.1 $cm^3/g$ | | 107[d] | *J. Am. Chem. Soc*., 2012, **134**, 17380-17383. |
| PCP-1 | 56.5 g $L^{-1}$ | | | | *Chem. Sci.*, 2014, **5**, 660-666 |
| $Zn_2(atz)_2(oba)$ | 80.6 $cm^3/g$ | 55.2 $cm^3/g$ | | | *Cryst. Growth Des*., 2013, **13**, 2118-2123. |
| mmen-CuBTTri | | 4.2 mmol/g | | 327 | *Energy Environ. Sci*., 2011, **4**, 3030-3040. |
| $Mg_2$(dobpdc) | | 6.42 mmol/g | | 200 | *J. Am. Chem. Soc*., 2012, ***134***, 7056-7065. |
| CALF-32 ($BF_4$) | 1.5 mmol $g^{-1}$ | | | | *Inorg. Chem. Front*., 2014, **1,** 302-305. |
| BILP-11 | 5.06 mmol $g^{-1}$ | | 7.6 | 56 (0.05 bar) | *J. Mater. Chem. A*, 2014, **2**, 12492-12500. |
| $[Co_2(pbdc)_2(bimb)_2(bimb)_{0.5}$ | 48.8 | 28.2 $cm^3/g$ | 5 | 19 | *J. Mater. Chem. A*, 2014, **2**, 12413-12422. |
| NOP-20 | 11.8 wt% | 7.2 wt% | | | *J. Mater. Chem. A*, 2014, **2**, 7795 - 7801. |
| ZIF-300 | | 40 $cm^3/cm^{-3}$ | | 22[b] | *Angew. Chem. Int. Ed*., 2014, **53**, 1-5. |

[a] Selectivity of $CO_2$ over $CH_4$ or $N_2$ when the gas phase mole fractions is 5/95;

[b] Selectivity of $CO_2$ over $CH_4$ $N_2$ when the gas phase mole fractions is 50/50;

[c] Selectivity of $CO_2$ over $N_2$ predicted when the gas phase mole fractions is 15/85;

[d] Calculated from pure component isotherms by Henry's law.

## References


1 (a) G. M. Sheldrick, SHELXS-97, Programs for X-ray Crystal Structure Solution, University of Göttingen, Göttingen, Germany, 1997; (b) G. M. Sheldrick, SHELXL-97, Programs for X-ray Crystal Structure Refinement, University of Göttingen, Göttingen, Germany, 1997; (c) L. J. Farrugia, WINGX, A Windows Program for Crystal Structure Analysis, University of Glasgow; Glasgow, UK, 1988.

2 A. L. Spek, *J. Appl. Crystallogr*., 2003, **36**, 7.

3 A. L. Myers and J. M. Prausnitz, *AIChE J.*, 1965, **11**, 121.

4 R. Krishna and J. R. Long, *J. Phys. Chem. C*, 2011, ***115***, 12941.

5 R. Krishna, *Microporous Mesoporous Mater.* 2014, ***185***, 30.

6 D. L Chen, H. Shang, W. Zhu and R. Krishna, *Chem. Eng. Sci.,* 2014, ***117***, 407.

7 D. L. Chen, N. Wang, F. F.Wang, J. Xie, Y. Zhong, W. Zhu, J. K. Johnson, and R. Krishna, *J. Phys. Chem. C*, 2014, ***118***, 17831.